Cellular/Molecular

Ca^{2+} Influx through NMDA-Gated Channels Activates ATP-Sensitive K^+ Currents through a Nitric Oxide–cGMP Pathway in Subthalamic Neurons

Ke-Zhong Shen[1] **and Steven W. Johnson**[1,2]

[1]Department of Neurology, Oregon Health and Science University, Portland, Oregon 97239, and [2]Portland Veterans Affairs Medical Center, Portland, Oregon 97207

Excessive burst firing of action potentials in subthalamic nucleus (STN) neurons has been correlated with the bradykinesia and rigidity seen in Parkinson's disease. Consequently, there is much interest in characterizing mechanisms that promote burst firing, such as the regulation of NMDA receptor function. Using whole-cell recording techniques in rat brain slices, we report that inward currents evoked by NMDA are greatly potentiated by ATP-sensitive K^+ (K-ATP) channel blocking agents in STN neurons but not in dopamine neurons in the substantia nigra. Moreover, we found that the ability of NMDA to evoke K-ATP current was blocked by inhibitors of nitric oxide synthase, guanylyl cyclase, and calcium/calmodulin. By altering firing patterns of STN neurons, this NMDA/K-ATP interaction may exert an important influence on basal ganglia output and thereby affect the clinical expression of Parkinson's disease.

Introduction

The subthalamic nucleus (STN) is composed of glutamate-containing neurons that regulate the output from the basal ganglia (Smith and Parent, 1988; Parent and Hazrati, 1995). As such, the STN is poised to exert powerful influences on muscle tone and movement. Dysfunction of STN output has been linked to the choreiform movements that are seen in Huntington's disease, as well as the restriction of movement that characterizes Parkinson's disease (Albin, 1995). Although overall neuronal activity has an important influence on behavior, it is now widely accepted that change in the firing pattern of STN neurons exerts a more important influence on motor function than does alterations in absolute firing rate (Bergman et al., 1998; Bevan et al., 2002). In particular, the chronic dopamine depletion seen in Parkinson's disease has been shown to promote burst discharges in STN neurons (Bergman et al., 1994; Ni et al., 2001). Moreover, changes in firing pattern in STN neurons correlate with the bradykinesia and tremor that are typical of Parkinson's disease (Magariños-Ascone et al., 2000; Benedetti et al., 2004). It stands to reason that membrane properties and neurotransmitter systems that influence firing patterns of STN neurons will likely play important roles in the clinical manifestations of movement disorders.

Activation of NMDA receptors has been shown to induce burst firing in many central neurons such as those in the spinal cord (Grillner and Wallén, 1985; Grubb et al., 1996), hypothalamus (Hu and Bourque, 1992), substantia nigra (Johnson et al., 1992; Overton and Clark, 1997), and many cells in the brainstem (Tell and Jean, 1991; Serafin et al., 1992; Kim and Chandler, 1995). In addition, previous studies by our laboratory have shown that NMDA evokes excitatory currents and promotes burst firing in STN neurons (Zhu et al., 2004, 2005). NMDA receptors are ionotropic glutamate-gated channels that have high permeability for Na^+ and Ca^{2+} (Mayer and Westbrook, 1987). Furthermore, NMDA receptor-gated channels are somewhat unusual in that they are subject to voltage-dependent block by Mg^{2+} at membrane potentials that are more hyperpolarized than the firing threshold of the cell (Ascher and Nowak, 1988). As a consequence, NMDA-gated currents show a region of negative slope conductance that typically occurs in the voltage range of -50 to -90 mV. Computer modeling studies have demonstrated that this region of negative slope conductance is critical for the generation of membrane oscillations that underlie burst firing (Li et al., 1996; Canavier, 1999).

Our laboratory has published several studies on the actions of NMDA on neurons in the STN and in dopamine neurons of the substantia nigra zona compacta (SNC). Using whole-cell recording techniques in rat brain slice preparations, we made the anecdotal observation that inward currents evoked by NMDA in STN neurons are generally much smaller than those that are evoked by the same concentrations of NMDA in SNC dopamine neurons (Wu and Johnson, 1996; Zhu et al., 2004). The purpose of the present study was to systematically characterize the voltage dependence of NMDA-gated currents in STN neurons and compare results with those recorded in substantia nigra neurons. Surprisingly, we found that the current–voltage (I–V) relationship for NMDA current in STN neurons lacked a well defined region of negative slope conductance that is so characteristic of NMDA-gated currents in other neurons. Moreover, we found

Received July 6, 2009; revised Oct. 6, 2009; accepted Nov. 9, 2009.

This work was supported by National Institutes of Health Grant NS38715 and the Portland Veterans Affairs Parkinson's Disease Research, Education, and Clinical Center. We also thank Dr. Anne I. Taupignon for helpful comments on the data.

Correspondence should be addressed to Dr. Ke-Zhong Shen, Department of Neurology, Oregon Health and Science University, Portland, OR 97239. E-mail: shenk@ohsu.edu.

DOI:10.1523/JNEUROSCI.3200-09.2010

 0270-6474/10/301882-12$15.00/0

that superfusing the slice preparation with an ATP-sensitive K^+ (K-ATP) channel blocker such as tolbutamide greatly increased NMDA inward currents in STN neurons and conferred a region of negative slope conductance to the *I–V* plot. In contrast, tolbutamide had no effect on the *I–V* relationship for NMDA-evoked currents in SNC dopamine neurons. In the present study, we report on second-messenger systems that mediate the activation of K-ATP channels by NMDA receptor stimulation in STN neurons. We suggest that this NMDA/K-ATP interaction is likely to exert an important influence on the excitability and firing pattern of STN neurons.

Materials and Methods

Tissue preparation. Horizontal slices containing diencephalon and rostral midbrain were prepared from male Sprague Dawley rats (Harlan) as described previously (Shen and Johnson, 2000). Adult rats (120–180 g) were used for STN and SNC recordings, whereas young rats (11–26 d old) were used to record from substantia nigra zona reticulata (SNR) neurons. Briefly, rats were anesthetized with isoflurane and killed by severing major thoracic vessels in accordance with institutional guidelines. Brains were rapidly removed, and slices were cut with a vibratome in an ice-cold sucrose buffer solution of the following composition (in mM): 187 sucrose, 2.5 KCl, 3.5 $MgCl_2$, 0.5 $CaCl_2$, 1.2 NaH_2PO_4, 20 glucose, and 26 $NaHCO_3$ (equilibrated with 95% O_2–5% CO_2). A slice containing the STN and SNR was then placed on a supporting net and submerged in a continuously flowing solution (2 ml/min) of the following composition (in mM): 126 NaCl, 2.5 KCl, 2.4 $CaCl_2$, 1.2 $MgCl_2$, 1.2 NaH_2PO_4, 19 $NaHCO_3$, and 11 glucose, pH 7.4 (gassed with 95% O_2 and 5% CO_2 at 36°C). Using a dissection microscope for visual guidance, the STN was located as gray matter ~2.7 mm lateral to the midline and 2 mm rostral to the center of the SNR.

Electrophysiological recordings. Whole-cell recordings were made with pipettes containing the following (in mM): 138 potassium gluconate, 2 $MgCl_2$, 1 $CaCl_2$, 0.2 EGTA, 10 HEPES, 1.5 ATP, and 0.3 GTP, pH 7.3. Pipette resistance ranged from 3 to 8 MΩ, whereas series resistance typically ranged from 15 to 40 MΩ. Membrane currents were recorded under voltage clamp and amplified with an Axopatch-1D amplifier. Baseline holding potentials were −70 mV in STN and SNR neurons and −60 mV in SNC neurons so that holding currents were close to 0. In some experiments, we used a "loose-patch" method to record extracellular currents and potentials (Nunemaker et al., 2003). For loose-patch recordings, patch pipettes were filled with standard extracellular solution; loose-patch recordings were made with a seal resistance typically 5–10 times the starting value of electrode resistance (3–8 MΩ). Data were acquired using a personal computer with a Digidata analog/digital interface and analyzed using pClamp software (Molecular Devices). Currents and potentials were recorded continuously using a MacLab analog/digital interface, Chart software (AD Instruments), and a Macintosh computer (Apple Computers). Membrane potentials for whole-cell recordings have been corrected for the liquid junction potential (10 mV).

Current–voltage studies. I–V relationships were constructed using either a series of hyperpolarizing voltage steps or a continuous voltage ramp. Using the voltage step method, currents were measured during a series of seven or eight hyperpolarizing voltage steps (400 ms duration) with 10 mV increments from a holding potential of −70 mV in STN and SNR cells or −60 mV in SNC neurons. Currents were measured immediately after capacitive transients to minimize the influence of hyperpolarization-activated cation currents. When using the voltage ramp method, currents were recorded during a slow voltage ramp (60 mV in 5 s) beginning at −140 mV in STN and SNR neurons or from −120 mV in SNC neurons. Slope conductance was calculated for each cell as the slope of a straight line in the *I–V* plot at voltages between −70 and −100 mV (or from −60 to −80 mV for SNC neurons). Mean slope conductance and SEM were obtained by averaging slope conductances from all cells. In some figures, *I–V* plots were displayed as "subtracted" currents in which currents recorded during the experimental treatment had been subtracted from those currents recorded in control. Therefore, these subtracted currents represent "net" currents that were produced or blocked by an experimental treatment.

Synaptic currents. Bipolar stimulation electrodes (tip separation, 300–500 μm) were placed in the slice 300 μm rostral to the STN. Synaptic currents were evoked by rectangular pulses (0.1 ms duration) of constant current that were either delivered as a single pulse every 10 s or by trains of pulses (100–200 Hz) lasting 50–1000 ms. To isolate synaptic currents mediated by NMDA receptors, slices were perfused with 6-cyano-7-nitro-quinoxalone (CNQX) (10 μM) and either bicuculline methiodide (30 μM) or picrotoxin (100 μM) to block AMPA and $GABA_A$ receptors, respectively. At the end of each experiment, we confirmed that the synaptic current was mediated by NMDA receptors by superfusing with the NMDA receptor antagonist (±)-2-amino-5-phosphonopentanoic acid (AP-5) (50 μM). Synaptic currents were recorded with voltage clamped at −70 mV.

Drugs and chemicals. All drugs were dissolved in aqueous or dimethylsulfoxide stock solutions. Most drugs were added to the slice superfusate. Stock solutions were diluted at least 1:1000 to the desired concentration in superfusate immediately before use. Approximately 30 s were required for the drug solution to enter the recording chamber; this delay was attributable to passage of the superfusate through a heat exchanger. In some experiments, NMDA was applied locally by pressure ejection from a micropipette. The tip of the micropipette containing NMDA (100 μM) was positioned above the brain slice within 100 μm of the recording pipette; the solution was ejected by pressure (500 ms duration) using a Picospritzer II (General Valve). LY83583 (6-anilino-5,8-quinolinequinone), AP-5, 7-NINA (7-nitroindazole monosodium salt), carboxy-PTIO [2-(4-carboxyphenyl)-4,4,5,5-tetramethylimidazoline-1-oxyl-3-oxide], ODQ (1*H*-[1,2,4]oxadiazolo[4,3-a]quinoxalin-1-one), calmidazolium, CGS9343B (1,3-dihydro-1-[1-[(4-methyl-4*H*,6*H*-pyrrolo[1,2-a][4,1]be nzoxazepin-4-yl)methyl]-4-piperidinyl]-2*H*-benzimidazol-2-one maleate), and glibenclamide were obtained from Tocris Bioscience. Tetrodotoxin (TTX), NMDA, apamin, AMPA, L-arginine, N^G-nitro-L-arginine methyl ester hydrochloride (L-NAME), AP-5, CNQX, bicuculline, tolbutamide, bepridil, picrotoxin, and $BaCl_2$ were obtained from Sigma-Aldrich.

Data analysis. Numerical data in the text and error bars in figures are expressed as mean ± SEM. Whenever possible, differences in *I–V* plots were analyzed using two-way ANOVA with repeated measures, followed by the Holm–Sidak pairwise comparison test (SigmaStat; Jandel Scientific). Otherwise, data were analyzed by paired *t* tests. Slope conductances and reversal potentials were calculated by linear regression of the *I–V* relationship for each cell; mean and SEM values were calculated by averaging the results from all cells in each experimental group.

Results

NMDA evokes a conductance increase in STN neurons

Members of our laboratory have reported previously that superfusing the brain slice with NMDA evokes burst firing of action potentials in both STN neurons and in SNC dopamine neurons (Johnson et al., 1992; Zhu et al., 2004). However, we also noted that inward currents evoked by NMDA are much more robust in SNC neurons compared with those in STN neurons. For example, in the present study, 10 μM NMDA evoked in SNC neurons an inward current of 108 ± 16 pA when measured at −60 mV ($n = 10$). In contrast, a higher concentration of NMDA (20 μM) evoked only 1 ± 5 pA of inward current in STN neurons when recorded at nearly the same voltage (−70 mV; $n = 65$). To investigate the voltage dependence of NMDA-evoked currents in STN neurons, we constructed *I–V* plots as shown in Figure 1*A*. Using continuous voltage ramps, we recorded currents before and during superfusion with NMDA (20 μM). By subtracting control currents from those recorded during NMDA superfusion, we constructed voltage plots for net currents evoked by NMDA as shown in Figure 1*B*. Of note, the *I–V* relationship illustrated in Figure 1*B* fails to show a region of negative slope conductance that typically characterizes NMDA-gated currents in other cen-

tral neurons (Mayer and Westbrook, 1987). By averaging reversal potentials in voltage ramp *I–V* plots from individual STN neurons, this yielded a mean reversal potential of −59.7 ± 2.4 mV ($n = 65$), which is a much more hyperpolarized value than the reversal potential of ~0 mV that would be typical for NMDA-evoked currents in other central neurons (Ascher and Nowak, 1988). These data suggest that NMDA-gated currents in STN neurons are mediated by an unusual combination of ionic components.

We also studied the voltage dependence of NMDA currents when recorded during a series of hyperpolarizing voltage steps, as illustrated in Figure 1*C*. Using this method, the *I–V* plot for net (subtracted) NMDA currents in Figure 1*D* shows that NMDA currents produce positive slope conductance at all test potentials. On average, NMDA-evoked currents in STN neurons were associated with a positive slope conductance of 2.41 ± 0.30 nS ($n = 65$) when measured between −70 and −100 mV. In the presence of TTX (0.5 μM), NMDA (20 μM) evoked currents with a positive slope conductance of 2.27 ± 0.34 nS ($n = 32$), which was not significantly different from control (two-way repeated measures ANOVA) (Fig. 1*D*). Finally, the NMDA receptor antagonist AP-5 (50 μM) completely blocked the action of NMDA ($n = 5$) (Fig. 1*D*). These results suggest that the NMDA-evoked conductance increase is not mediated indirectly by the release of neurotransmitters or other substances within the brain slice.

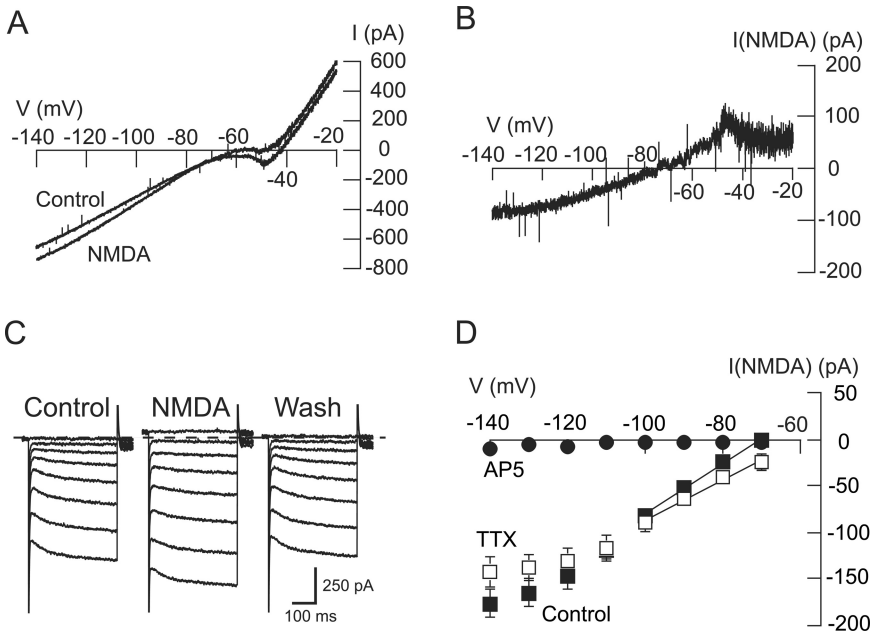

Figure 1. NMDA increases conductance in STN neurons. ***A***, *I–V* plots from an STN neuron recorded using depolarizing voltage ramps before (control) and during (20 μM) application of NMDA. ***B***, Net currents evoked by NMDA, which were calculated by subtracting currents recorded in the control condition from those recorded in NMDA. Data were obtained from the same neuron as shown in ***A***. Note that subtracted NMDA current has a positive slope conductance between voltages of −50 and −80 mV, which is unusual for NMDA-evoked current. ***C***, Current traces recorded during a series of hyperpolarizing voltage steps (from −70 to −140 mV) show that NMDA (20 μM) increases membrane conductance in an STN neuron. Dashed line indicates 0 current. ***D***, Summarized *I–V* plots showing net (subtracted) currents evoked by NMDA in the control condition ($n = 65$), in the presence of TTX (0.5 μM; $n = 32$), and in the presence of AP-5 (50 μM; $n = 5$,). Note that AP-5 completely blocked NMDA-evoked currents, whereas TTX had no significant effect. Solid lines in these and subsequent *I–V* plots represent slope conductances that were calculated by linear regression for currents between −70 and −100 mV.

NMDA-evoked conductance increase is blocked by Ba^{2+}

To test for involvement of K^+ in the NMDA-dependent conductance increase, we investigated the ability of Ba^{2+} to modify NMDA currents in STN neurons. In the control current trace shown in Figure 2*A*, NMDA (20 μM) evoked a small inward current followed by an outward current when recorded at −70 mV. However, NMDA evoked a much larger inward current after the brain slice was superfused for 7 min with Ba^{2+} (300 μM). On average, NMDA evoked 6 ± 20 pA of outward current at −70 mV under control conditions ($n = 8$). In the presence of Ba^{2+}, however, NMDA caused an inward current of 174 ± 43 pA in those same neurons ($p < 0.01$, paired *t* test). Ba^{2+} also greatly modified the NMDA *I–V* relationship. As seen in Figure 2*B*, Ba^{2+} converted a fairly linear positive slope conductance increase to 1 that clearly shows a region of negative slope conductance between the voltages of −70 and −90 mV. Figure 2*C* shows averaged current–voltage plots for net NMDA currents recorded before (control) and during Ba^{2+} superfusion. Under the control condition, the NMDA-evoked current was associated with a positive slope conductance of 2.89 ± 0.92 nS ($n = 8$), but in the presence of Ba^{2+} (300 μM), the NMDA-evoked current was changed significantly to a negative slope conductance of 0.79 ± 0.36 nS ($p < 0.01$, paired *t* test). Net NMDA currents blocked by Ba^{2+} (300 μM), which were calculated by subtracting net NMDA currents in Ba^{2+} from those recorded under control conditions, had an estimated reversal potential of −102 ± 7 mV, which is close to the expected K^+ equilibrium potential (−101 mV) as predicted by the Nernst equation. These data suggest that stimulation of NMDA receptors evokes a K^+ current. Moreover, we suggest that this increase in a K^+ conductance prevents the appearance of the region of negative slope conductance that is typically associated with NMDA-gated current.

NMDA evokes sulfonylurea-sensitive currents in STN neurons

To further characterize the K^+ current that is activated by NMDA, we tested the effects of K-ATP blocking drugs on NMDA-gated currents. We first tested the ability of the sulfonylurea agent tolbutamide to modify the action of NMDA. In the control current trace shown in Figure 3*A*, NMDA (20 μM) evoked a small inward current (at −70 mV) in this STN neuron. However, this inward current was greatly increased after superfusing the slice with tolbutamide (100 μM) for 10 min. On average, NMDA produced an inward current of 102 ± 12 pA in the presence of tolbutamide, which was significantly different from the 4 ± 11 pA of outward current that was evoked by NMDA under the control condition ($p < 0.001$, paired *t* test; $n = 27$). As shown in Figure 3*B*, tolbutamide also significantly altered the voltage dependence of NMDA currents ($p < 0.05$, two-way repeated measures ANOVA; $n = 27$). Under the control condition, NMDA current was associated with a positive slope conductance of 2.80 ± 0.42 nS, and extrapolation of these data yielded an estimated reversal potential of −61 ± 4 mV ($n = 27$). In contrast, NMDA-evoked currents in tolbutamide had a characteristic negative slope conductance of 1.01 ± 0.16 nS ($p < 0.0001$, paired *t*

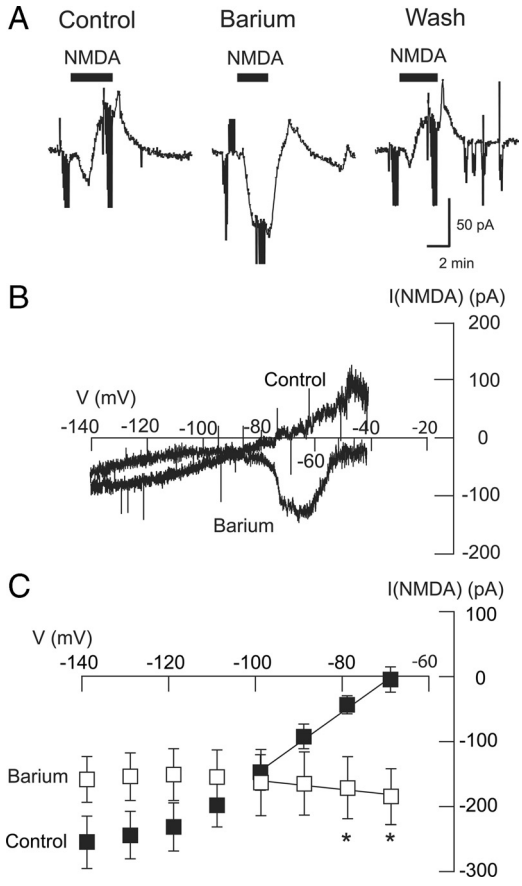

Figure 2. Barium sensitivity of the NMDA-evoked conductance increase. ***A***, Current traces show that Ba^{2+} (300 μM) increases the inward current evoked by NMDA (20 μM) recorded at a holding potential of −70 mV. Note that Ba^{2+} also significantly reduced the outward current that followed the inward current. Truncated downward deflections in current records are artifacts caused by voltage steps that were used to measure series resistance or membrane currents. ***B***, *I–V* plots of net (subtracted) NMDA current recorded from an STN neuron in the control condition and in the presence of Ba^{2+} (300 μM). Note that application of Ba^{2+} (300 μM) changed the slope of *I–V* plots from positive to negative between the voltages of −60 and −80 mV. ***C***, Summarized plots show that Ba^{2+} significantly changed the slope conductance of NMDA-evoked currents from positive to negative ($n = 8$). Asterisks indicate significant differences ($p < 0.05$; paired *t* test).

test). NMDA currents that were blocked by tolbutamide (100 μM), which were calculated by subtracting net NMDA currents in the presence of tolbutamide from those under control conditions, had an estimated reversal potential of −99 ± 18 mV that was close to the expected K^+ equilibrium potential. Tolbutamide also had no effect on either the amplitude or slope of the conductance of currents evoked by AMPA (0.6 μM; $n = 5$).

To evaluate the specificity of this effect of tolbutamide, we examined the actions of the K-ATP blockers bepridil (10 μM) and glibenclamide (1 μM) on NMDA-evoked currents. Bepridil significantly altered the current evoked by 20 μM NMDA from a control outward current of 8 ± 11 pA to an inward current of 86 ± 13 pA ($p < 0.05$, paired *t* test; $n = 4$). Bepridil also altered the slope of NMDA conductance from a positive slope conductance of 1.86 ± 0.94 nS under the control condition to a negative slope conductance of 1.00 ± 0.11 nS in the presence of bepridil ($p < 0.05$, paired *t* test; $n = 4$). Similarly, glibenclamide increased NMDA inward current at −70 mV from a control value of 16 ± 21 to 86 ± 15 pA ($p < 0.05$, paired *t* test; $n = 4$). Glibenclamide also altered the slope of NMDA conductance from positive (2.79 ± 0.91 nS) to negative (0.78 ± 0.25 nS; $p < 0.05$; $n = 4$). In contrast, apamin (100 nM), which blocks small-conductance Ca^{2+}-activated K^+ (gKCa) channels, had no effect on inward currents evoked by NMDA at −70 mV (42 ± 6 pA control compared with 24 ± 6 pA in apamin; $p > 0.05$, paired *t* test; $n = 4$). Apamin also had no effect on NMDA slope conductance (+0.92 ± 0.27 nS control compared with +0.82 ± 0.21 nS; $p > 0.05$, paired *t* test; $n = 4$). These results suggest that the K^+ current evoked by NMDA is mediated by K-ATP channels but not by small-conductance gKCa channels.

Effects of ATP regeneration solution

Because K-ATP channels are characterized by their sensitivity to being blocked by intracellular ATP (Stanfield, 1987), we next investigated whether or not loading the cell with ATP could prevent activation of K-ATP currents by NMDA. We recorded whole-cell currents with pipettes that contained an ATP-regeneration solution that was composed of ATP (10 mM), creatine phosphate (20 μM), phosphocreatine kinase (50 U/ml), and $MgCl_2$ (6 mM) (Forscher and Oxford, 1985). We used this ATP regeneration solution because the addition of creatine phosphate and phosphocreatine kinase has been shown to more effectively maintain ATP activity than can be achieved by simply raising the concentration of ATP in the pipette solution (Rosenmund and Westbrook, 1993). After recording with the ATP regeneration solution for at least 20 min, NMDA (20 μM) caused an inward current of 62 ± 22 pA (at −70 mV) that was associated with a negative slope conductance of 0.79 ± 0.24 nS when measured between −70 and −100 mV ($n = 3$). The presence of negative slope conductance in the NMDA current–voltage relationship suggests that K-ATP currents that would have been evoked by NMDA are blocked by elevated levels of intracellular ATP.

Lack of tolbutamide-sensitive NMDA currents in SNC neurons

Thus far, the above data suggest that NMDA receptor stimulation can evoke K-ATP currents. To investigate whether or not this phenomenon is unique to STN neurons, we tested the ability of tolbutamide to affect NMDA-gated currents in dopamine SNC neurons. As shown in the current traces in Figure 3*C*, tolbutamide (100 μM) failed to increase inward currents evoked by NMDA (10 μM) in this SNC neuron. On average, NMDA produced an inward current of 204 ± 35 pA at −60 mV in the presence of tolbutamide, which was not significantly different from the 182 ± 33 pA of inward current that was evoked by NMDA under the control condition ($p > 0.05$, paired *t* test; $n = 7$). As shown in the *I–V* plot in Figure 3*D*, NMDA (10 μM) evoked currents in SNC neurons with a negative slope conductance of 6.1 ± 1.5 nS when measured between −60 and −80 mV ($n = 7$). Moreover, this slope conductance was not significantly different when recorded in the presence of tolbutamide (6.8 ± 1.3 nS; $p > 0.05$, paired *t* test). By averaging reversal potentials in voltage ramp *I–V* plots from individual SNC neurons under control conditions, this yielded a mean reversal potential for NMDA current of −4.3 ± 7.8 mV ($n = 3$), which is similar to values reported for other central neurons (Ascher and Nowak, 1988). These results suggest that NMDA does not evoke K-ATP currents in SNC dopamine neurons.

We also measured NMDA-induced currents in SNR neurons. Recorded at −70 mV, NMDA (10 μM) evoked an inward current of 276 ± 52 pA (at −70 mV). Furthermore, currents evoked by NMDA in SNR cells had a characteristic negative slope conductance of 5.6 ± 1.2 nS when measured between −70 and −100 mV ($n = 7$). Although we cannot conclude that activation of K-ATP

channels by NMDA is unique to STN neurons, these data demonstrate that this phenomenon is not shared by all central neurons.

K-ATP channels are activated by extrasynaptic NMDA receptors

To explore the location of NMDA receptors that activate K-ATP channels, we compared the effect of tolbutamide on currents evoked by local application of NMDA with those evoked by electrical stimulation of the brain slice. Figure 4*A* shows the effect of NMDA that was applied locally by pressure ejection from a micropipette that was placed close to the recording pipette. Under the control condition, local application of NMDA evoked an inward current that was followed by an outward current. However, Figure 4*A* shows that tolbutamide (100 μM) greatly increased the NMDA-dependent inward current and abolished the outward current. On average, tolbutamide increased the inward current evoked by local application of NMDA by 261 ± 32% and completely abolished the rebound outward current ($n = 6$). In contrast, Figure 4*B* shows the effect of tolbutamide on synaptic currents that were mediated by NMDA receptors. In these experiments, a single electrical stimulus was delivered to the brain slice while recording from a nearby STN neuron. The slice superfusate contained CNQX (10 μM) and bicuculline (30 μM) to block AMPA and $GABA_A$ receptors, respectively, but, as seen in Figure 4*B*, tolbutamide (100 μM) failed to affect synaptic currents mediated by NMDA receptors ($n = 11$). Tolbutamide also failed to affect membrane currents evoked by trains of electrical stimuli. As shown in Figure 4*C*, a train of 10 stimuli delivered at 200 Hz evoked a robust AP-5-sensitive inward current, whereas tolbutamide (100 μM) had no effect ($n = 10$). In contrast, repetitive trains of stimuli successfully evoked a tolbutamide- or AP-5-sensitive outward current in 13 of 23 STN neurons, as shown in Figure 4, *D* and *E*. In these experiments, three to five trains of high-frequency stimulation (HFS) at 100 Hz for 1 s were delivered to the slice every 20 s in the presence of CNQX (10 μM) and picrotoxin (100 μM), according to the method of Hopper and Garthwaite (2006). As shown in Figure 4*D*, HFS evoked 34 ± 6 pA of outward current under control conditions, which was reduced to 2 ± 3 pA by 100 μM tolbutamide ($p < 0.001$, paired *t* test; $n = 8$). As shown in Figure 4*E*, AP-5 (50 μM) also reduced the HFS-induced outward current to 2 ± 3 pA, from a control value of 30 ± 11 pA ($p < 0.05$, paired *t* test; $n = 5$). Although it is possible that repetitive HFS evokes K-ATP current via intense stimulation of synaptic NMDA receptors, the sum of our data is most consistent with the hypothesis that extrasynaptic NMDA receptors, as opposed to those located within the synapse, are responsible for K-ATP channel activation.

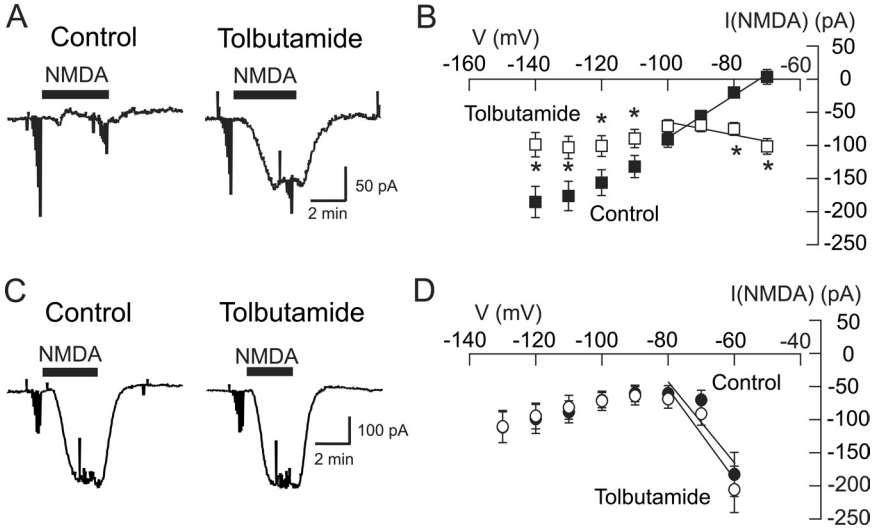

Figure 3. Tolbutamide blocks the NMDA-evoked conductance increase in STN neurons (***A***, ***B***) but not in SNC neurons (***C***, ***D***). ***A***, Current traces recorded at −70 mV show that application of tolbutamide (100 μM) increased the amplitude of inward currents evoked by NMDA (20 μM) in an STN neuron. ***B***, Summarized NMDA *I–V* plots for STN neurons show that tolbutamide (100 μM) significantly altered the *I–V* plot compared with control ($p < 0.05$, two-way repeated measures ANOVA). *$p < 0.05$, significant differences at specific test potentials (Holm–Sidak pairwise comparison test). ***C***, In an SNC neuron, tolbutamide (100 μM) has no effect on current evoked by NMDA (10 μM) recorded at −60 mV. ***D***, Summarized data show that tolbutamide failed to modify voltage-dependent NMDA currents in SNC neurons ($n = 7$).

Nitric oxide mediates the NMDA-dependent K-ATP conductance increase

It is well established that K-ATP channel activation is facilitated by nitric oxide (NO) (Miyoshi et al., 1994; Shinbo and Iijima, 1997; Brito et al., 2006). Moreover, NMDA receptor stimulation has been shown to activate nitric oxide synthase (NOS) (Snyder, 1992; Sattler et al., 1999; Hopper and Garthwaite, 2006). Therefore, we investigated the possibility that activation of NOS underlies the NMDA-dependent increase in K-ATP conductance. As seen in the current traces in Figure 5*A*, superfusing the slice with the NOS inhibitor L-NAME (200 μM) for 15 min greatly potentiated inward current evoked by NMDA (20 μM) at −70 mV. In the presence of L-NAME, NMDA produced an average inward current of 79 ± 11 pA at −70 mV, which was significantly different from the 32 ± 17 pA of outward current that was produced by NMDA under the control condition in these same neurons ($p < 0.05$, paired *t* test; $n = 14$). L-NAME also changed the voltage dependence of NMDA currents, as shown in Figure 5*B*. Under control conditions, current evoked by NMDA was associated with a positive slope conductance of 3.79 ± 0.99 nS; extrapolation of these data yielded an estimated reversal potential of −65.2 ± 6.0 mV ($n = 14$). However, in the presence of L-NAME, the NMDA *I–V* plot had a negative slope conductance of 0.71 ± 0.15 nS, which was significantly different from the control value ($p < 0.001$, paired *t* test). Moreover, the voltage dependence of NMDA currents was significantly different in L-NAME compared with control ($p < 0.05$, two-way repeated measures ANOVA). Tolbutamide-sensitive NMDA currents, which were calculated by subtracting net NMDA currents in the presence of tolbutamide from those under control conditions, had a reversal potential of −100 ± 3 mV, which is close to the K^+ equilibrium potential as predicted by the Nernst equation.

We also tested the effect of the NOS inhibitor 7-NINA on NMDA currents. As shown in Figure 5*C*, superfusing 7-NINA (100 μM) for 15 min greatly potentiated inward current evoked by NMDA (20 μM) at −70 mV. In the presence of 7-NINA, NMDA produced an average inward current of 50 ± 6 pA, which was significantly different from the 6 ± 9 pA of outward current that was produced by NMDA under control conditions in these same neurons ($p < 0.05$, paired *t* test; $n = 9$). As seen in Figure 5*D*, 7-NINA also significantly changed the voltage dependence of net NMDA currents ($p < 0.01$, two-way repeated measures

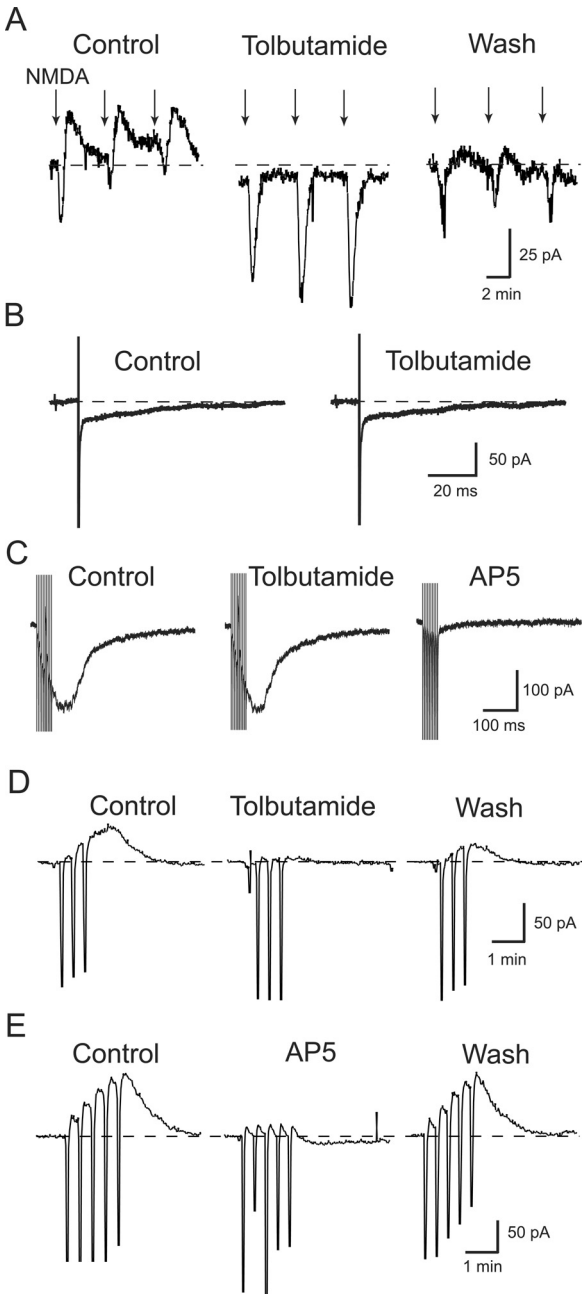

Figure 4. Effects of tolbutamide (100 μM) on NMDA receptor-mediated currents. ***A***, Tolbutamide potentiates inward currents and blocks outward currents evoked by local application of NMDA. Currents were evoked in an STN neuron by pressure ejection of 100 μM NMDA (arrows) from a micropipette placed near the recording patch pipette. Note that outward currents follow NMDA-induced inward currents during control recordings. ***B***, Tolbutamide has no effect on an NMDA receptor-mediated EPSC evoked in an STN neuron by focal electrical stimulation of the brain slice. This EPSC, recorded in CNQX (10 μM) and bicuculline (30 μM), was completely blocked by 50 μM AP-5 (data not shown). ***C***, A train of 10 stimuli delivered at 200 Hz evokes AP-5-sensitive inward current but tolbutamide has no effect. ***D***, Three trains of HFS consisting of stimuli delivered at 100 Hz for 1 s every 20 s evoke a tolbutamide-sensitive outward current. Downward deflections are artifacts caused by HFS. ***E***, Five trains of HFS evoke an outward current that is blocked by AP-5 (50 μM). Each recording was from a different STN neuron.

ANOVA). Under control conditions, NMDA current was associated with a positive slope conductance of 2.05 ± 0.48 nS. However, in the presence of 7-NINA (100 μM), net NMDA current had a negative slope conductance of 0.60 ± 0.12 nS in these same cells ($p < 0.0001$, paired *t* test; $n = 9$).

Finally, we tested whether or not the specific NO scavenger carboxy-PTIO could mimic the actions of NOS inhibitors on NMDA currents. As shown in the current traces in Figure 5*E*, superfusing carboxy-PTIO (100 μM) for 15 min greatly potentiated inward current evoked by NMDA (20 μM) at −70 mV. In the presence of carboxy-PTIO, NMDA produced an average inward current of 63 ± 2 pA, which was significantly larger than the 1 ± 15 pA of inward current that was produced by NMDA at −70 mV under control conditions in these same neurons ($p < 0.05$, paired *t* test; $n = 5$). As seen in Figure 5*F*, carboxy-PTIO also significantly changed the voltage dependence of net NMDA currents ($p < 0.01$, two-way repeated measures ANOVA). Under control conditions, NMDA current was associated with a positive slope conductance of 2.16 ± 0.84 nS. However, in the presence of carboxy-PTIO (100 μM), net NMDA current had a negative slope conductance of 0.71 ± 0.13 nS in these same cells ($p < 0.01$, paired *t* test; $n = 5$). These data support the hypothesis that NO acts as a second messenger to mediate the activation of K-ATP channels by NMDA receptor stimulation.

L-Arginine mimics NMDA by activating K-ATP current

To further support a role for NO, we next explored the ability of the NO substrate L-arginine to mimic NMDA in activating K-ATP channels. As seen in the current traces in Figure 6*A*, L-arginine (10 mM) evoked a tolbutamide-sensitive outward current at −70 mV. On average, superfusing the slice with L-arginine (10 mM) evoked 28 ± 9 pA of outward current at −70 mV. However, in the presence of tolbutamide (100 μM), L-arginine actually evoked 11 ± 2 pA of inward current in these same neurons ($p < 0.05$, paired *t* test; $n = 7$). The voltage dependence of L-arginine-induced currents and their block by tolbutamide is shown in the *I–V* plot in Figure 6*B*. The net L-arginine current blocked by tolbutamide reversed direction at −101 ± 7 mV, which is close to the K^+ equilibrium potential as predicted by the Nernst equation. The L-arginine-induced outward current was also blocked by the NOS inhibitor L-NAME (100 μM). Measured at −70 mV, L-arginine (10 mM) evoked an inward current of 23 ± 5 pA in the presence of L-NAME, which was significantly different from the 41 ± 18 pA of outward current evoked by L-arginine (10 mM) in the control condition ($p < 0.05$, paired *t* test; $n = 4$). As shown in Figure 6*C*, L-NAME also significantly altered the *I–V* relationship for L-arginine-evoked currents ($p < 0.05$, two-way repeated measures ANOVA; $n = 4$). Net L-arginine currents blocked by L-NAME reversed direction at −106 ± 4 mV, which is close to the predicted K^+ equilibrium potential. These data suggest that L-arginine evokes a tolbutamide-sensitive current that is mediated by NO. Furthermore, these data support the hypothesis that endogenous NO is required for the K-ATP conductance increase produced by NMDA receptor activation in STN neurons.

Role of guanylyl cyclase in K-ATP activation

Because actions of NO on K-ATP channels can be mediated by activation of cGMP-dependent protein kinase (Han et al., 2001; Brito et al., 2006), we next investigated the role of cGMP in NMDA-dependent K-ATP currents. As seen in the current traces in Figure 7*A*, NMDA (20 μM) evoked a small inward current at −70 mV that was greatly increased by superfusing the slice with the guanylyl cyclase inhibitor ODQ (100 μM). On average, NMDA evoked a small net outward current of 6 ± 30 pA under the control condition ($n = 6$). However, NMDA evoked 107 ± 19 pA of inward current at −70 mV in the presence of ODQ in these same cells ($p < 0.05$, paired *t* test). The voltage dependence of the

effect of ODQ on NMDA currents is shown in the *I–V* plot in Figure 7*B*. Under the control condition, NMDA evoked currents with a positive slope conductance of 2.72 ± 0.54 nS. However, in the presence of ODQ, NMDA currents were evoked with a negative slope conductance of 0.33 ± 0.13 nS ($p < 0.01$, paired *t* test). Moreover, a two-way repeated measures ANOVA test showed that the NMDA *I–V* relationships were significantly different in ODQ compared with control ($p < 0.001$). We also explored effects of the guanylyl cyclase inhibitor LY83583. When recorded at −70 mV, LY83583 (20 μM) significantly increased the inward current evoked by NMDA (20 μM) from a control value of 16 ± 24 to 200 ± 39 pA ($p < 0.05$, paired *t* test; $n = 5$). Moreover, LY83583 significantly altered the voltage dependence of NMDA-evoked currents, as shown in Figure 7*C* ($p < 0.05$, two-way repeated measures ANOVA; $n = 5$). Under control conditions, NMDA evoked currents with a positive slope conductance of 2.83 ± 0.74 nS ($n = 5$). However, in the presence of LY83583 (20 μM), NMDA current had a negative slope conductance of 0.84 ± 0.61 nS in these same neurons ($p < 0.01$, paired *t* test). These results suggest that a cGMP-dependent pathway mediates the activation of K-ATP channels by NMDA receptor stimulation.

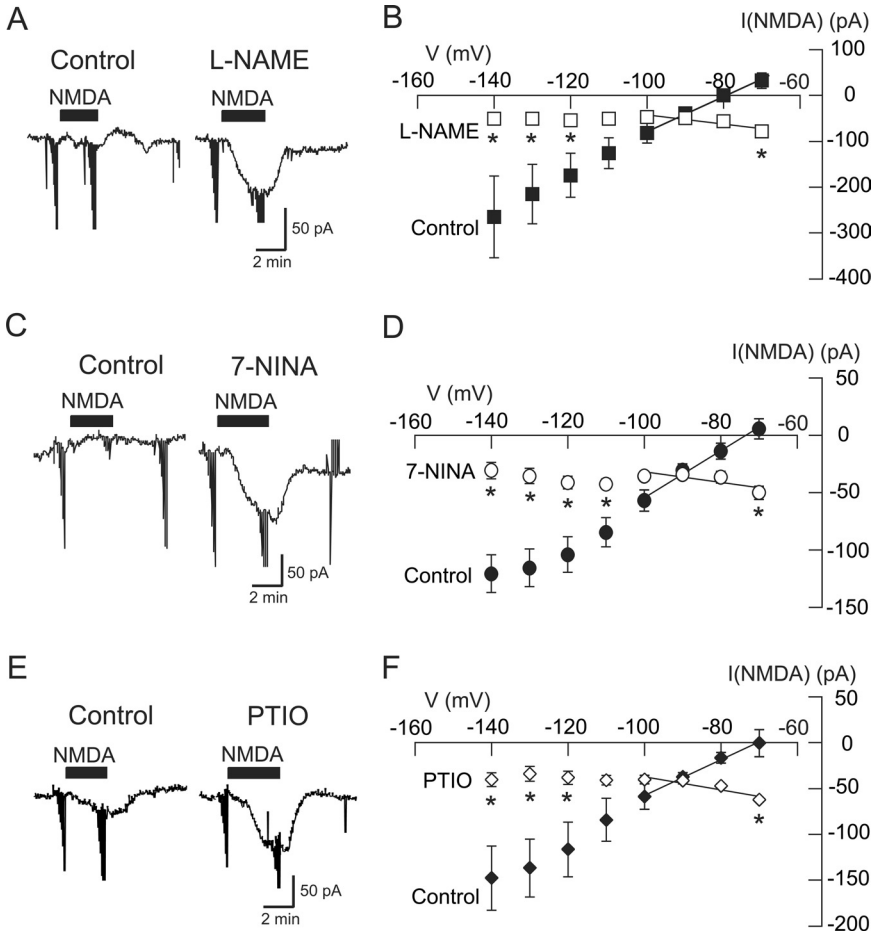

Figure 5. The NMDA-evoked K-ATP conductance increase requires NO. ***A***, Current traces show that the NOS inhibitor L-NAME (200 μM) increased the amplitude of inward current evoked by NMDA (20 μM) at −70 mV. ***B***, Summarized *I–V* plots of net NMDA currents show that L-NAME (200 μM) significantly increased the amplitude of inward currents evoked by NMDA at −70 mV and reduced the slope conductance ($n = 14$). ***C***, Current traces show that the NOS inhibitor 7-NINA (100 μM) increased the amplitude of inward currents evoked by NMDA (20 μM) at −70 mV. ***D***, Summarized *I–V* plots of NMDA currents show that 7-NINA (100 μM) significantly increased the amplitude of inward currents evoked by NMDA at −70 mV and reduced slope conductance ($n = 9$). ***E***, Current traces show that the NO scavenger carboxy-PTIO (100 μM) increased the amplitude of inward currents evoked by NMDA (20 μM) at −70 mV. ***F***, Summarized *I–V* plots of NMDA current show that carboxy-PTIO (100 μM) significantly increased the amplitude of inward currents evoked by NMDA at −70 mV and reduced the slope conductance ($n = 5$). *$p < 0.05$ (two-way repeated measures ANOVA with Holm–Sidak pairwise comparison test).

Ca^{2+} influx is required for NMDA-evoked K-ATP conductance increase

Because calcium/calmodulin is a known activator of NOS (Snyder, 1992), we explored whether or not Ca^{2+} influx through NMDA-gated ion channels might be necessary for activation of K-ATP channels. We made whole-cell recordings with pipettes that contained BAPTA (10 mM), which has much faster Ca^{2+}-buffering kinetics than the EGTA that we normally used in our internal pipette solution (Nichols and Suplick, 1996). We then tested the effect of a low Ca^{2+} solution (0.2 mM) on NMDA current. As shown in the current traces in Figure 8*A*, superfusing the slice with the low Ca^{2+} solution significantly increased the inward current evoked by NMDA (20 μM) at −70 mV. Under control conditions (2.4 mM Ca^{2+} in superfusate), NMDA evoked a small outward current of 2 ± 16 pA at −70 mV ($n = 5$). However, in 0.2 mM Ca^{2+}, NMDA evoked a large inward current of 197 ± 26 pA in the same cells ($p < 0.01$, paired *t* test). As shown in Figure 8*B*, the low Ca^{2+} solution caused a significant change in the NMDA *I–V* relationship ($p < 0.001$, two-way repeated measures ANOVA; $n = 5$). In the control condition, NMDA current had a positive slope conductance of 3.34 ± 1.14 nS, but when recording in the low Ca^{2+} solution, NMDA current had a negative slope conductance of 0.68 ± 0.63 nS ($p < 0.01$, paired *t* test; $n = 5$). These results suggest that Ca^{2+} influx through NMDA-gated channels plays a role in activation of K-ATP currents.

To explore a role for calmodulin, we performed experiments with the calmodulin inhibitors CGS9343B (10–40 μM) and calmidazolium (10–20 μM). When recorded at −70 mV, NMDA (20 μM) evoked 43 ± 14 pA of inward current in the presence of CGS9343B compared with an outward current of 45 ± 27 pA under the control condition ($p < 0.01$, paired *t* test; $n = 6$) (Fig. 8*C*). Moreover, CGS9343B altered the NMDA *I–V* relationship ($p = 0.056$, two-way repeated measures ANOVA) (Fig. 8*D*). In the control condition, NMDA current had a positive slope conductance of 4.37 ± 0.98 nS, but when recording in the presence of CGS9343B, NMDA current had a significantly smaller positive slope conductance of 0.53 ± 0.32 nS ($p < 0.01$, paired *t* test; $n = 6$). We obtained similar results with calmidazolium. On average, NMDA (20 μM) evoked 3 ± 16 pA of outward current at −70 mV ($n = 9$), but in the presence of calmidazolium, NMDA evoked an average inward current of 87 ± 25 pA in these same neurons ($p < 0.01$, paired *t* test) (Fig. 8*E*). Calmidazolium also modified the NMDA *I–V* relationship (Fig. 8*F*). In the presence of calmidazolium, NMDA current had a slope conductance of 0.01 ± 0.64 nS, which was significantly different from the positive slope conduc-

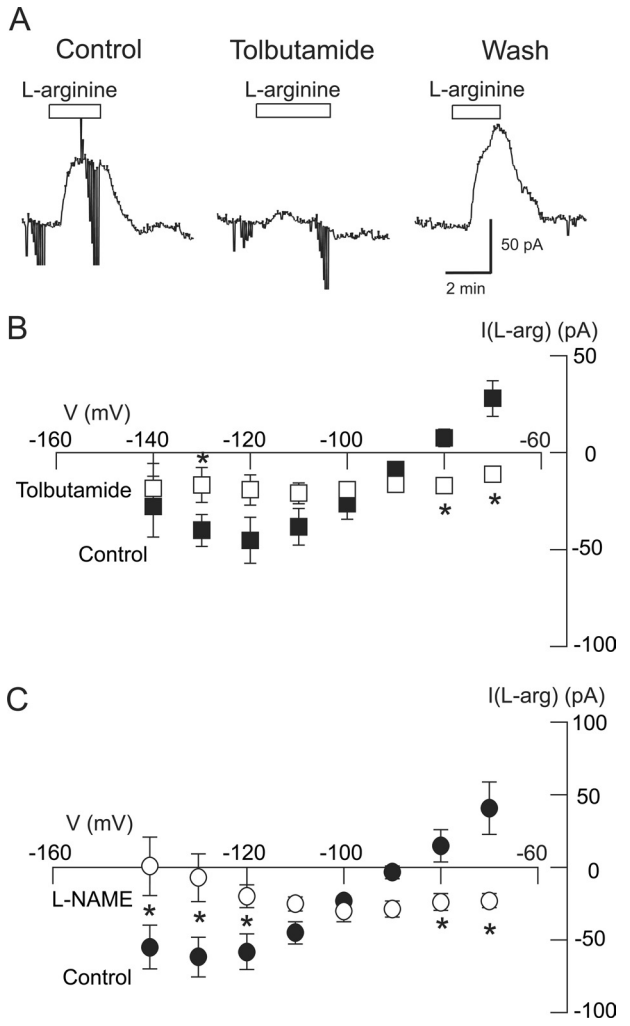

Figure 6. L-arginine evokes K-ATP currents in STN neurons. ***A***, Current traces show that application of the NOS substrate L-arginine (10 mM) evokes a tolbutamide (100 μM)-sensitive outward current at −70 mV. ***B***, *I–V* plots show that net (subtracted) currents evoked by L-arginine are antagonized by tolbutamide ($n = 7$). ***C***, Current–voltage plots show that net (subtracted) currents evoked by L-arginine are antagonized by the NOS inhibitor L-NAME (200 μM; $n = 4$). *$p < 0.05$ (two-way repeated measures ANOVA with Holm–Sidak pairwise comparison test).

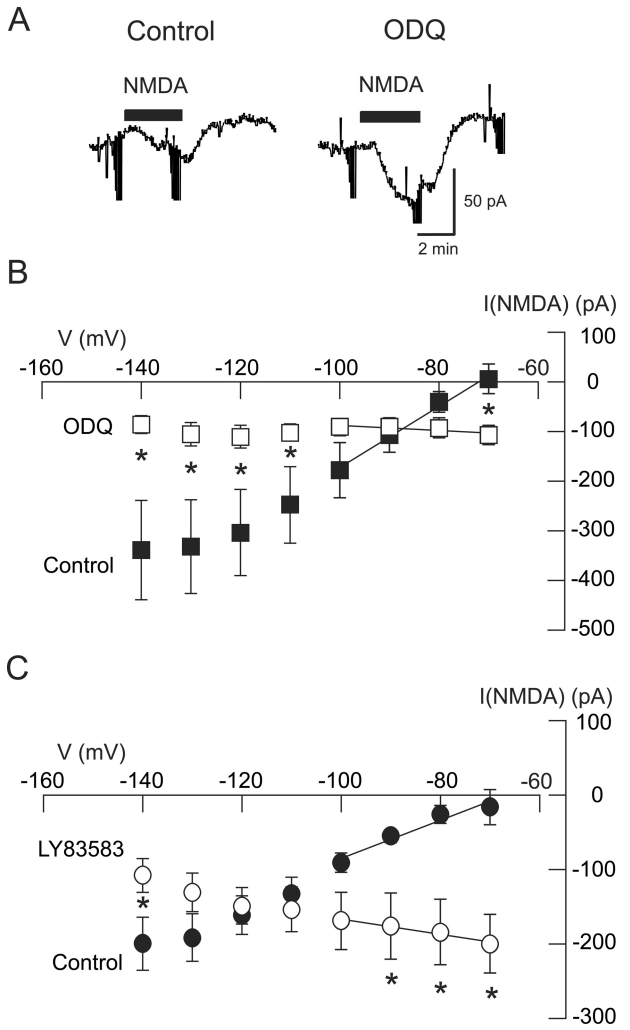

Figure 7. The NMDA-evoked K-ATP conductance increase requires activation of a cGMP-dependent pathway. ***A***, Current traces show that the guanylyl cyclase inhibitor ODQ (100 μM) greatly increased the inward current evoked by NMDA (20 μM) recorded at −70 mV. ***B***, Summarized *I–V* plots show that the increase in conductance evoked by NMDA is significantly antagonized by ODQ ($n = 6$). ***C***, Summarized *I–V* plots show that the selective guanylyl cyclase inhibitor LY83583 (20 μM) significantly antagonized the conductance increase evoked by NMDA ($n = 5$). *$p < 0.05$ (two-way repeated measures ANOVA with Holm–Sidak pairwise comparison test).

tance of 3.09 ± 0.67 nS in the control condition ($p < 0.01$, paired *t* test; $n = 9$). These results are consistent with the hypothesis that Ca^{2+} influx and activation of calmodulin are required for NMDA-dependent activation of K-ATP channels.

Functional consequences of K-ATP channel activation

If NMDA receptor stimulation causes coactivation of K-ATP channels, what might be the resulting impact on firing frequency and firing pattern? To investigate effect on firing rate, we used the loose-patch recording technique to record extracellular action potentials in STN neurons (Nunemaker et al., 2003). Under control conditions, a 5 min superfusion with NMDA caused a significant increase in firing rate, from a control value of 9.9 ± 1.5 to 22.2 ± 4.9 Hz ($p < 0.05$, paired *t* test; $n = 8$) (Fig. 9*A*). However, in tolbutamide (100 μM), NMDA caused a much larger increase in firing rate, to 35.0 ± 6.8 Hz ($p < 0.001$, paired *t* test), compared with NMDA alone, in these same neurons. Interestingly, tolbutamide alone caused a small increase in spontaneous firing rate (from 9.9 ± 1.5 to 12.1 ± 2.6 Hz), but this was not statistically significant ($p = 0.0599$, paired *t* test; $n = 8$). These data, which are summarized in Figure 9*B*, show that block of K-ATP channels greatly potentiates the excitatory effect of NMDA on firing rate. By using the loose-patch technique, these data also show that the NMDA/K-ATP interaction persists when intracellular contents are not dialyzed by whole-cell patch solutions.

To evaluate changes in firing pattern, we examined the influences of NMDA and tolbutamide on the depolarization-induced plateau potential that underlies one type of burst firing in STN neurons (Beurrier et al., 1999; Bevan and Wilson, 1999; Baufreton et al., 2003). As shown in Figure 10*A*, a brief depolarizing current pulse evokes a burst of spikes that rides on top of a plateau potential. Although superfusion with NMDA (20 μM) alone does not significantly alter plateau potential duration, NMDA causes a marked prolongation of plateau potential duration in the presence of tolbutamide (100 μM). These data are summarized in Figure 10*B*. In the presence of tolbutamide, NMDA increased the average plateau potential duration from a control duration of

382 ± 55 to 2169 ± 419 ms in the same STN neurons ($p < 0.01$, paired t test; $n = 8$). Interestingly, tolbutamide alone also produced a small but significant prolongation of plateau potential duration, from a control value of 237 ± 36 to 382 ± 55 ms ($p < 0.05$); this finding signifies the presence of baseline K-ATP channel activity. In summary, these results demonstrate that K-ATP currents that are activated by NMDA receptor stimulation exert significant influences over firing rate and firing pattern of STN neurons.

Discussion

Our results have shown that inward currents evoked by NMDA are markedly potentiated by K-ATP channel blocking agents in STN neurons but not in SNC dopamine neurons. Sulfonylurea-sensitive currents evoked by NMDA were blocked by NOS inhibitors and were mimicked by L-arginine, suggesting that K-ATP channel activation was mediated by NO. Furthermore, we found that guanylyl cyclase inhibitors prevented NMDA from evoking sulfonylurea-sensitive currents. Finally, we provided evidence that K-ATP channel activation by NMDA was dependent on Ca^{2+} influx and activation of calmodulin. These data suggest that Ca^{2+} influx through NMDA-gated channels activates K-ATP currents in STN neurons by NO- and cGMP-coupled mechanisms.

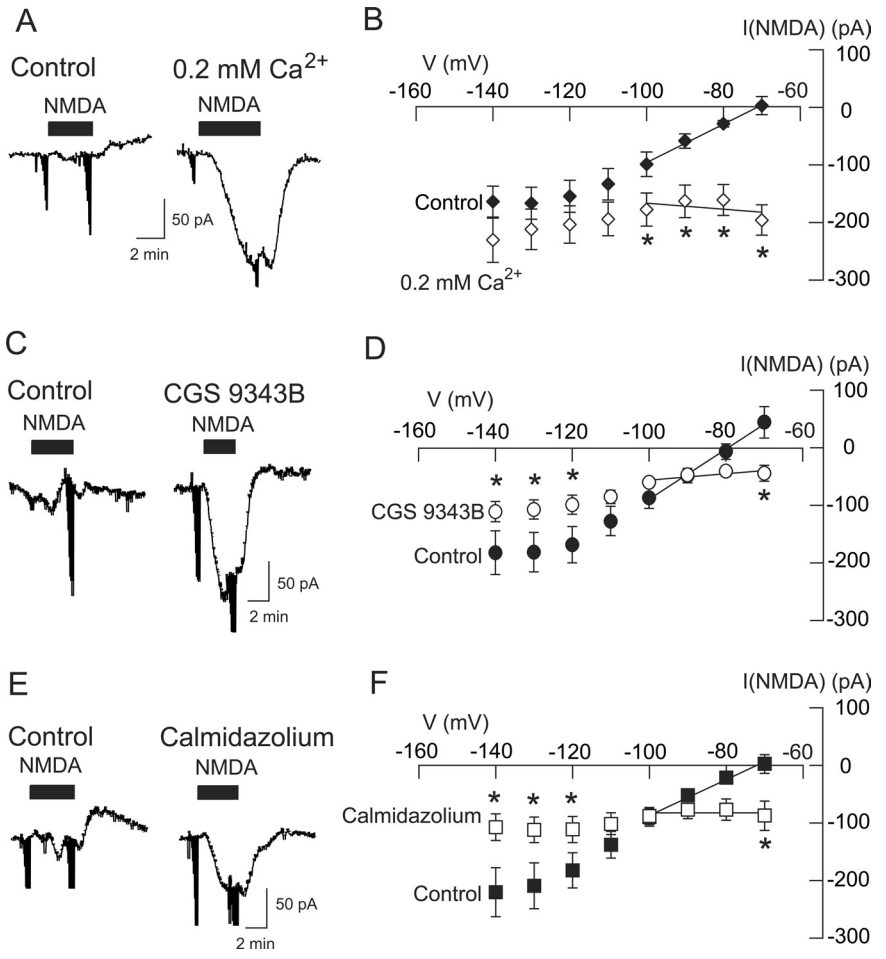

Figure 8. The NMDA-induced K-ATP conductance increase is Ca^{2+} and calmodulin dependent. ***A***, Current traces show that superfusion with a low Ca^{2+} (0.2 mM) bath solution increased the amplitude of inward currents evoked by NMDA at −70 mV. ***B***, Summarized *I–V* plots show that superfusion with low Ca^{2+} (0.2 mM) significantly reduced the conductance increase evoked by NMDA ($n = 5$). Recordings were performed with pipette solutions that contained BAPTA in place of EGTA. ***C***, Current traces show that the calmodulin inhibitor CGS9343B (40 μM) augments inward current evoked by NMDA at −70 mV. ***D***, Summarized *I–V* plots show that superfusion with CGS9343B reduced the conductance increase that was evoked by NMDA ($n = 6$). ***E***, Current traces show that the calmodulin inhibitor calmidazolium (20 μM) augments NMDA-induced inward currents at −70 mV. ***F***, Summarized *I–V* plots show that superfusion with calmidazolium reduced the conductance increase that was evoked by NMDA ($n = 9$). *$p < 0.05$ (two-way repeated measures ANOVA with Holm–Sidak pairwise comparison test).

Coupling of NMDA receptors to K-ATP channels

It is well known that NMDA receptor stimulation can generate NO by Ca^{2+}-dependent activation of NOS (Snyder, 1992; Sattler et al., 1999; Hopper and Garthwaite, 2006). Moreover, it is also well established that K-ATP channel opening can be greatly facilitated by NO-mediated activation of cGMP-dependent protein kinase (Shinbo and Iijima, 1997; Han et al., 2001; Brito et al., 2006). Thus, it is somewhat surprising that NMDA receptor-dependent activation of K-ATP channels is not a more commonly observed phenomenon. Nevertheless, Philip and Armstead (2004) reported that NMDA caused dilatation of pial arterioles by activation of a sulfonylurea-sensitive mechanism, which was presumed to be mediated by NO. Also, Kwiecien et al. (1993) reported that tolbutamide augmented NMDA inward currents in hippocampal neurons, although they also reported that this phenomenon was not K^+ dependent, as would have been expected if tolbutamide potentiated NMDA currents by blocking K-ATP outward current. In addition, Grabb and Choi (1999) found that repeated exposure of cultured cerebral cortical neurons to low concentrations of NMDA protected against hypoxic/ischemic cell death, and this neuroprotective effect was thought to be mediated at least in part by activation of K-ATP channels. Thus, there are several studies in the literature that would suggest that NMDA-dependent activation of K-ATP channels might be a more widespread phenomenon that is generally thought.

Lack of NMDA/K-ATP coupling in substantia nigra neurons

Given the fact that neurons from the substantia nigra are known to express high levels of K-ATP channel subunits (Liss et al., 1999; Velísek et al., 2008), it is interesting that we found no evidence that NMDA receptor stimulation evoked K-ATP currents in these cells. Although a study by Giustizieri et al. (2007) reported that the NMDA blocker memantine prevented hypoxia-induced K-ATP currents in SNC dopamine neurons, the K-ATP current was not thought to be evoked by NMDA receptor stimulation because the block of K-ATP currents by memantine persisted in the presence of MK-801 [(+)-5-methyl-10,11-dihydro-5*H*-dibenzo [a,d] cyclohepten-5,10-imine maleate] and other NMDA antagonists. In a study that is clearly relevant to the present, Webb et al. (1996) reported that superfusion with NMDA evoked a tolbutamide-sensitive hyperpolarization in SNC dopamine neurons in slices of guinea pig midbrain. Although this result is consistent with our results in STN neurons, their recordings were made in a "phasic" subtype of neuron located in the rostral SNC that exhibited characteristics that are unusual for dopamine neurons, such as narrow action potentials, absence of H-current, and little post-

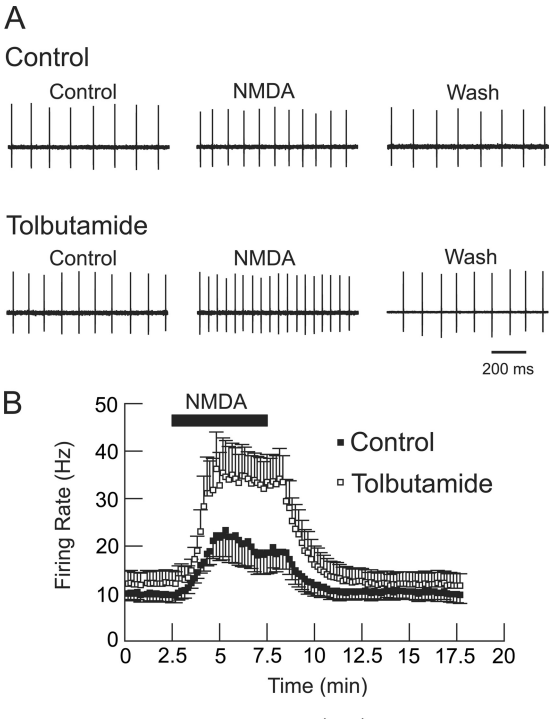

Figure 9. Loose-patch recordings of STN neurons showing tolbutamide (100 μM)-induced augmentation of the acceleration in firing rate produced by NMDA (20 μM). ***A***, Single-cell action potentials recorded extracellularly from an STN neuron in the presence of NMDA with and without tolbutamide. Note that the excitatory effect of NMDA is more pronounced in the presence of tolbutamide. ***B***, Averaged responses from eight STN neurons. Note the significant increase in NMDA-dependent firing rate produced by tolbutamide superfusion ($p < 0.001$, paired *t* test; $n = 8$). Tolbutamide-alone produced a small increase in firing rate, but this was not statistically significant ($p = 0.0599$).

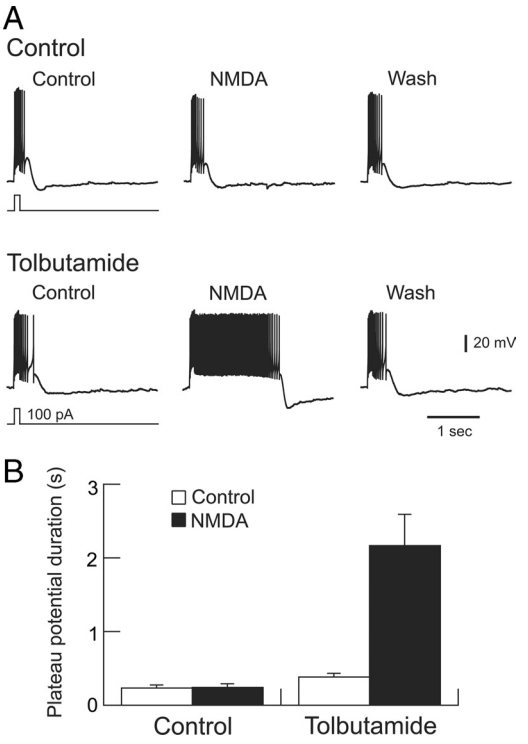

Figure 10. Block of K-ATP channels potentiates the ability of NMDA to prolong plateau potentials. ***A***, Current-clamp whole-cell recordings of an STN neuron showing the effects of NMDA (20 μM) in the presence and absence of tolbutamide (100 μM). A brief depolarizing current was applied as indicated to evoke plateau potentials. All voltage traces are from the same STN neuron. Note that NMDA greatly prolonged the duration of the plateau potential in the presence of tolbutamide. A small hyperpolarizing holding current was applied to establish an initial membrane potential of −75 mV. ***B***, Summary graph showing prolongation of plateau potential duration by NMDA in the presence of tolbutamide ($p < 0.01$, paired *t* test; $n = 8$). Tolbutamide alone also produced a small but significant increase in plateau potential duration ($p < 0.05$, paired *t* test).

spike hyperpolarization (Nedergaard and Greenfield, 1992). Thus, it is not clear that all types of dopamine neuron in the guinea pig brain would show this NMDA/K-ATP interaction. Perhaps subcellular proximity of NMDA receptors to K-ATP channels is necessary for NMDA/K-ATP interactions, and this may be is a significant cell-dependent variable. It is also possible that species differences could be important in determining whether or not NMDA receptors couple to K-ATP channels.

Extrasynaptic versus synaptic NMDA receptors

Our results showed that K-ATP currents are activated by local application of NMDA, whereas K-ATP current was not evoked after a single EPSC or train of HFS. These data suggest that extrasynaptic NMDA receptors are responsible for K-ATP channel activation. Although we could evoke K-ATP currents with HFS that was repeated every 20s (Fig. 4*D*,*E*), the underlying mechanism is uncertain. One might consider the possibility that repetitive HFS evokes K-ATP current by allowing glutamate to spill over to extrasynaptic NMDA receptors. However, a single burst of HFS should also permit glutamate spillover, and yet K-ATP current was not evoked (Fig. 4*C*). Moreover, the 20 s interval between each HFS should allow sufficient time for glutamate uptake by transporters, which would make accumulation of extracellular glutamate unlikely (Clements et al., 1992). Conversely, repetitive HFS might evoke K-ATP current by causing glial release of glutamate onto extrasynaptic NMDA receptors, such as has been described in hippocampal brain slices after intense stimulation of Schaffer collaterals (Fellin et al., 2004). Finally, it is possible that repetitive HFS activates synaptic NMDA receptors to cause a slow buildup of intracellular Ca^{2+} in STN neurons that eventually triggers K-ATP activation via the NOS/cGMP second-messenger system. Although the precise mechanism that underlies K-ATP activation by repetitive HFS is not known, our data are most consistent with the hypothesis that K-ATP currents are evoked by stimulation of extrasynaptic NMDA receptors that are located far from the synapse.

K-ATP channel activation by ATP depletion

It is well established that K-ATP channels can be opened by intracellular ATP depletion (Belles et al., 1987; Röper and Ashcroft, 1995). Thus, one might consider the possibility that NMDA evokes K-ATP current in STN neurons by depleting ATP levels by either excessive activation of Na^+/K^+-ATPase (Lees, 1991) or Ca^{2+}-dependent suppression of ATP synthase (Budd and Nicholls, 1996). However, our standard internal pipette solution contained 1.5 mM ATP, which makes it unlikely that brief exposure to NMDA would cause significant ATP depletion. Although studies in cultured neurons have shown that NMDA treatment can cause ATP depletion, these studies used relatively high concentrations of NMDA that were applied for longer periods of time compared with parameters used in our experiments (Novelli et al., 1988; Meli et al., 2004). Moreover, NMDA-induced ATP depletion is more easily accomplished when NMDA is used with a model of energy depletion such as glucose deprivation (Czyz et al., 2002). Because our studies used brief exposures of NMDA in superfu-

sate or local application by micropipette while recording with pipettes containing ATP, it is unlikely that acute ATP depletion can account for the generation of K-ATP currents in STN neurons.

Role of Ca^{2} in K-ATP channel activation

Our results clearly suggest that Ca^{2+} influx through NMDA-gated channels activates second-messenger systems that cause K-ATP channel opening. However, it remains to be determined whether or not Ca^{2+} influx through NMDA channels is the only source of Ca^{2+} that can evoke K-ATP current. It is relevant to note that K-ATP activation in other cells commonly occurs in response to glucose deprivation, the presence of reactive oxygen species, or other examples of metabolic stress (Miki and Seino, 2005). In the STN neuron, buildup of intracellular Ca^{2+} might also be viewed as a metabolic stress that can trigger K-ATP channel opening. It will be important in future studies to establish whether or not other sources of Ca^{2+} influx, such as voltage-gated Ca^{2+} channels and transient receptor potential channels, might also evoke K-ATP current in STN neurons.

Functional considerations

It should be pointed out that the hyperpolarizing influence of K-ATP currents will tend to dampen the influence of NMDA receptor activation. Thus, it is possible that K-ATP channel activation would serve as a negative feedback inhibitor to prevent excessive excitation caused by glutamate release. It is also worth noting that K-ATP channel subunits have been shown to be up-regulated in the basal ganglia in the 6-hydroxydopamine rodent model of Parkinson's disease (Wang et al., 2005). Because basal ganglia output in Parkinson's disease is thought to be driven by excessive bursting activity of STN neurons (Bergman et al., 1994; Benedetti et al., 2004), others have suggested that K-ATP channel openers might be therapeutic in the treatment of Parkinson's disease (Maneuf et al., 1996; Wang et al., 2005). Indeed, our results on burst firing associated with plateau potentials suggests that K-ATP channel openers might curtail excessive burst firing that could be triggered by NMDA receptor stimulation. Future studies will be needed to explore the usefulness of K-ATP channel openers as a treatment of Parkinson's disease.

References

Albin RL (1995) The pathophysiology of chorea/ballism and parkinsonism. Parkinsonism Relat Dis 1:3–11.

Ascher P, Nowak L (1988) The role of divalent cations in the *N*-methyl-D-aspartate responses of mouse central neurones in culture. J Physiol 399:247–266.

Baufreton J, Garret M, Rivera A, de la Calle A, Gonon F, Dufy B, Bioulac B, Taupignon A (2003) D_5 (not D_1) dopamine receptors potentiate burst-firing in neurons of the subthalamic nucleus by modulating an L-type calcium conductance. J Neurosci 23:816–825.

Belles B, Hescheler J, Trube G (1987) Changes of membrane currents in cardiac cells induced by long whole-cell recordings and tolbutamide. Pflugers Arch 409:582–588.

Benedetti F, Colloca L, Torre E, Lanotte M, Melcarne A, Pesare M, Bergamasco B, Lopiano L (2004) Placebo-responsive Parkinson patients show decreased activity in single neurons of subthalamic nucleus. Nat Neurosci 7:587–588.

Bergman H, Wichmann T, Karmon B, DeLong MR (1994) The primate subthalamic nucleus. II. Neuronal activity in the MPTP model of parkinsonism. J Neurophysiol 72:507–520.

Bergman H, Feingold A, Nini A, Raz A, Slovin H, Abeles M, Vaadia E (1998) Physiological aspects of information processing in the basal ganglia of normal and parkinsonian primates. Trends Neurosci 21:32–38.

Beurrier C, Congar P, Bioulac B, Hammond C (1999) Subthalamic nucleus neurons switch from single-spike activity to burst-firing mode. J Neurosci 19:599–609.

Bevan MD, Wilson CJ (1999) Mechanisms underlying spontaneous oscillation and rhythmic firing in rat subthalamic neurons. J Neurosci 19:7617–7628.

Bevan MD, Magill PJ, Terman D, Bolam JP, Wilson CJ (2002) Move to the rhythm: oscillations in the subthalamic nucleus-external globus pallidus network. Trend Neurosci 25:525–531.

Brito GA, Sachs D, Cunha FQ, Vale ML, Lotufo CM, Ferreira SH, Ribeiro RA (2006) Peripheral antinociceptive effect of pertussis toxin: activation of the arginine/NO/cGMP/PKG/ATP-sensitive K^+ channel pathway. Eur J Neurosci 24:1175–1181.

Budd SL, Nicholls DG (1996) Mitochondria, calcium regulation, and acute glutamate excitotoxicity in cultured cerebellar granule cells. J Neurochem 67:2282–2291.

Canavier CC (1999) Sodium dynamics underlying burst firing and putative mechanisms for the regulation of the firing pattern in midbrain dopamine neurons: a computational approach. J Comput Neurosci 6:49–69.

Clements JD, Lester RA, Tong G, Jahr CE, Westbrook GL (1992) The time course of glutamate in the synaptic cleft. Science 258:1498–1501.

Czyz A, Baranauskas G, Kiedrowski L (2002) Instrumental role of Na^+ in NMDA excitotoxicity in glucose-deprived and depolarized cerebellar granule cells. J Neurochem 81:379–389.

Fellin T, Pascual O, Gobbo S, Pozzan T, Haydon PG, Carmignoto G (2004) Neuronal synchrony mediated by astrocytic glutamate through activation of extrasynaptic NMDA receptors. Neuron 43:729–743.

Forscher P, Oxford GS (1985) Modulation of calcium channels by norepinephrine in internally dialyzed avian sensory neurons. J Gen Physiol 85:743–763.

Giustizieri M, Cucchiaroni ML, Guatteo E, Bernardi G, Mercuri NB, Berretta N (2007) Memantine inhibits ATP-dependent K^+ conductances in dopamine neurons of the rat substantia nigra pars compacta. J Pharmacol Exp Ther 322:721–729.

Grabb MC, Choi DW (1999) Ischemic tolerance in murine cortical cell culture: critical role for NMDA receptors. J Neurosci 19:1657–1662.

Grillner S, Wallén P (1985) The ionic mechanisms underlying *N*-methyl-D-aspartate receptor-induced, tetrodotoxin-resistant membrane potential oscillations in lamprey neurons active during locomotion. Neurosci Lett 60:289–294.

Grubb BD, Riley RC, Hope PJ, Pubols L, Duggan AW (1996) The burst-like firing of spinal neurons in rats with peripheral inflammation is reduced by an antagonist of *N*-methyl-D-aspartate. Neuroscience 74:1077–1086.

Han J, Kim N, Kim E, Ho WK, Earm YE (2001) Modulation of ATP-sensitive potassium channels by cGMP-dependent protein kinase in rabbit ventricular myocytes. J Biol Chem 276:22140–22147.

Hopper RA, Garthwaite J (2006) Tonic and phasic nitric oxide signals in hippocampal long-term potentiation. J Neurosci 26:11513–11521.

Hu B, Bourque CW (1992) NMDA receptor-mediated rhythmic bursting activity in rat supraoptic nucleus neurones *in vitro.* J Physiol 458:667–687.

Johnson SW, Seutin V, North RA (1992) Burst firing in dopamine neurons induced by *N*-methyl-D-aspartate: role of electrogenic sodium pump. Science 258:665–667.

Kim YI, Chandler SH (1995) NMDA-induced burst discharge in guinea pig trigeminal motoneurons *in vitro.* J Neurophysiol 74:334–346.

Kwiecien R, Medina I, Barbin G, Ben-Ari Y (1993) The hypoglycemic sulphonylurea tolbutamide increases *N*-methyl-D-aspartate- but not kainate-activated currents in hippocampal neurons in culture. Eur J Pharmacol 249:325–329.

Lees GJ (1991) Inhibition of sodium-potassium-ATPase: a potentially ubiquitous mechanism contributing to central nervous system neuropathology. Brain Res Rev 16:283–300.

Li YX, Bertram R, Rinzel J (1996) Modeling *N*-methyl-D-aspartate-induced bursting in dopamine neurons. Neuroscience 71:397–410.

Liss B, Bruns R, Roeper J (1999) Alternative sulfonylurea receptor expression defines metabolic sensitivity of K-ATP channels in dopaminergic midbrain neurons. EMBO J 18:833–846.

Magariños-Ascone CM, Figueiras-Mendez R, Riva-Meana C, Córdoba-Fernández A (2000) Subthalamic neuron activity related to tremor and movement in Parkinson's disease. Eur J Neurosci 12:2597–2607.

Maneuf YP, Duty S, Hille CJ, Crossman AR, Brotchie JM (1996) Modulation of GABA transmission by diazoxide and cromakalim in the globus

pallidus: implications for the treatment of Parkinson's disease. Exp Neurol 139:12–16.

Mayer ML, Westbrook GL (1987) Permeation and block of *N*-methyl-D-aspartic acid receptor channels by divalent cations in mouse cultured central neurones. J Physiol 394:501–527.

Meli E, Pangallo M, Picca R, Baronti R, Moroni F, Pellegrini-Giampietro DE (2004) Differential role of poly(ADP-ribose) polymerase-1 in apoptotic and necrotic neuronal death induced by mild or intense NMDA exposure *in vitro*. Mol Cell Neurosci 25:172–180.

Miki T, Seino S (2005) Roles of K-ATP channels as metabolic sensors in acute metabolic changes. J Mol Cell Cardiol 38:917–925.

Miyoshi H, Nakaya Y, Moritoki H (1994) Nonendothelial-derived nitric oxide activates the ATP-sensitive K^+ channel of vascular smooth muscle cells. FEBS Lett 345:47–49.

Nedergaard S, Greenfield SA (1992) Sub-populations of pars compacta neurons in the substantia nigra: the significance of qualitatively and quantitatively distinct conductances. Neuroscience 48:423–437.

Ni ZG, Bouali-Benazzouz R, Gao DM, Benabid AL, Benazzouz A (2001) Time-course of changes in firing rates and firing patterns of subthalamic nucleus neuronal activity after 6-OHDA-induced dopamine depletion in rats. Brain Res 899:142–147.

Nichols RA, Suplick GR (1996) Rapid chelation of calcium entering isolated rat brain nerve terminals during stimulation inhibits neurotransmitter release. Neurosci Lett 211:135–137.

Novelli A, Reilly JA, Lysko PG, Henneberry RC (1988) Glutamate becomes neurotoxic via the *N*-methyl-D-aspartate receptor when intracellular energy levels are reduced. Brain Res 451:205–212.

Nunemaker CS, DeFazio RA, Moenter SM (2003) A targeted extracellular approach for recording long-term firing patterns of excitable cells: a practical guide. Biol Proceed Online 5:53–62.

Overton PG, Clark D (1997) Burst firing in midbrain dopaminergic neurons. Brain Res Rev 25:312–334.

Parent A, Hazrati LN (1995) Functional anatomy of the basal ganglia. II. The place of subthalamic nucleus and external pallidum in basal ganglia circuitry. Brain Res Rev 20:128–154.

Philip S, Armstead WM (2004) NMDA dilates pial arteries by K-ATP and K-Ca channel activation. Brain Res Bull 63:127–131.

Röper J, Ashcroft FM (1995) Metabolic inhibition and low internal ATP activate K-ATP channels in rat dopaminergic substantia nigra neurones. Pflugers Arch 430:44–54.

Rosenmund C, Westbrook GL (1993) Rundown of *N*-methyl-D-aspartate channels during whole-cell recording in rat hippocampal neurons: role of Ca^{2+} and ATP. J Physiol 470:705–729.

Sattler R, Xiong Z, Lu WY, Hafner M, MacDonald JF, Tymianski M (1999) Specific coupling of NMDA receptor activation to nitric oxide neurotoxicity by PSD-95 protein. Science 284:1845–1848.

Serafin M, Khateb A, de Waele C, Vidal PP, Mühlethaler M (1992) Medial vestibular nucleus in the guinea-pig: NMDA-induced oscillations. Exp Brain Res 88:187–192.

Shen KZ, Johnson SW (2000) Presynaptic dopamine D_2 and muscarine M_3 receptors inhibit excitatory and inhibitory transmission to rat subthalamic neurones *in vitro*. J Physiol 525:331–341.

Shinbo A, Iijima T (1997) Potentiation by nitric oxide of the ATP-sensitive K^+ current induced by K^+ channel openers in guinea-pig ventricular cells. Br J Pharmacol 120:1568–1574.

Smith Y, Parent A (1988) Neurons of the subthalamic nucleus in primates display glutamate but not GABA immunoreactivity. Brain Res 453:353–356.

Snyder SH (1992) Nitric oxide: first in a new class of neurotransmitters? Science 257:494–496.

Stanfield PR (1987) Nucleotides such as ATP may control the activity of ion channels. Trends Neurosci 10:335–339.

Tell F, Jean A (1991) Activation of *N*-methyl-D-aspartate receptors induces endogenous rhythmic bursting activities in nucleus tractus solitarii neurons: an intracellular study on adult rat brain stem slices. Eur J Neurosci 3:1353–1365.

Velísek L, Velísková J, Chudomel O, Poon KL, Robeson K, Marshall B, Sharma A, Moshé SL (2008) Metabolic environment in substantia nigra reticulata is critical for the expression and control of hypoglycemia-induced seizures. J Neurosci 28:9349–9362.

Wang S, Hu LF, Yang Y, Ding JH, Hu G (2005) Studies of ATP-sensitive potassium channels on 6-hydroxydopamine and haloperidol rat models of Parkinson's disease: implications for treating Parkinson's disease? Neuropharmacology 48:984–992.

Webb CP, Nedergaard S, Giles K, Greenfield SA (1996) Involvement of the NMDA receptor in a non-cholinergic action of acetylcholinesterase in guinea-pig substantia nigra pars compacta neurons. Eur J Neurosci 8:837–841.

Wu YN, Johnson SW (1996) Pharmacological characterization of inward current evoked by *N*-methyl-D-aspartate in dopamine neurons in the rat brain slice. J Pharmacol Exp Ther 279:457–463.

Zhu ZT, Munhall A, Shen KZ, Johnson SW (2004) Calcium dependent subthreshold oscillations determine bursting activity induced by *N*-methyl-D-aspartate in rat subthalamic neurons *in vitro*. Eur J Neurosci 19:1296–1304.

Zhu ZT, Munhall A, Shen KZ, Johnson SW (2005) NMDA enhances a depolarization-activated inward current in subthalamic neurons. Neuropharmacology 49:317–327.